BIOCHEMISTRY
including biophysical chemistry & molecular biology

Article

pubs.acs.org/biochemistry

# Design, Overexpression, and Purification of Polymerization-Blocked Yeast αβ-Tubulin Mutants

Vinu Johnson, Pelin Ayaz, Patrick Huddleston, and Luke M. Rice*

Department of Biochemistry, University of Texas Southwestern Medical Center, Dallas, Texas 75390, United States

**ABSTRACT:** Microtubule dynamics play essential roles in intracellular organization and cell division. They result from structural and biochemical properties of αβ-tubulin heterodimers and how these polymerizing subunits interact with themselves and with regulatory proteins. A broad understanding of the underlying mechanisms has been established, but fundamental questions remain unresolved. The lack of routine access to recombinant αβ-tubulin represents an obstacle to deeper insight into αβ-tubulin structure, biochemistry, and recognition. Indeed, the widespread reliance on animal brain αβ-tubulin means that very few in vitro studies have taken advantage of powerful and ordinarily routine techniques like site-directed mutagenesis. Here we report new methods for purifying wild-type or mutant yeast αβ-tubulin from inducibly overexpressing strains of *Saccharomyces cerevisiae*. Inducible overexpression is an improvement over existing approaches that rely on constitutive expression: it provides higher yields while also allowing otherwise lethal mutants to be purified. We also designed and purified polymerization-blocked αβ-tubulin mutants. These "blocked" forms of αβ-tubulin give a dominant lethal phenotype when expressed in cells; they cannot form microtubules in vitro and when present in mixtures inhibit the polymerization of wild-type αβ-tubulin. The effects of blocking mutations are very specific, because purified mutants exhibit normal hydrodynamic properties, bind GTP, and interact with a tubulin-binding domain. The ability to overexpress and purify wild-type αβ-tubulin, or mutants like the ones we report here, creates new opportunities for structural studies of αβ-tubulin and its complexes with regulatory proteins, and for biochemical and functional studies of microtubule dynamics and its regulation.

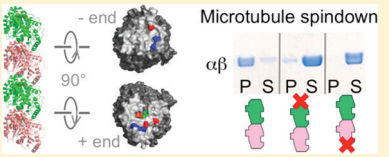


Microtubules are dynamic, hollow cylindrical polymers of αβ-tubulin that undergo dramatic rearrangements over the course of each cell cycle and are found in all dividing eukaryotic cells. Microtubules (MTs) facilitate their own remodeling by stochastically switching between growing and shrinking, a property known as dynamic instability (reviewed in ref 1). Dynamic instability is an intrinsic property of MTs that can be reconstituted in vitro[2−4] and is essential for proper MT function in vivo. Dynamic instability results from the self-interaction affinities of αβ-tubulin, an assembly-dependent GTPase activity, and multiple conformations of αβ-tubulin. It is regulated by a host of microtubule-associated proteins (MAPs).

Despite impressive progress, a comprehensive understanding of the structural and molecular mechanisms that generate and regulate dynamic instability remains elusive. Structural questions are an important part of the debate. For example, crystal structures define two conformations of αβ-tubulin in atomic detail,[5,6] but there is disagreement about which one represents the "ground state" conformation and how (if at all) the conformation of αβ-tubulin depends on the nucleotide bound to β-tubulin.[7−11] The paucity of structural information also limits our ability to understand how regulatory MAPs and drugs recognize αβ-tubulin and perhaps also control its conformation. Ultimately, the lack of structural insight undermines the understanding of function.

A fundamental obstacle that prevents more rapid progress is the near exclusive use of αβ-tubulin isolated from animal brain (where αβ-tubulin is abundant) for in vitro experiments. The widespread reliance on brain tubulin is in part explained by the failure of heterologous expression of αβ-tubulin in bacteria, likely because bacteria lack a number of dedicated chaperones that are required for the folding and assembly of αβ-tubulin heterodimers. Whatever the reasons, the lack of a routine, robust source of recombinant αβ-tubulin severely curtails the in vitro analysis of αβ-tubulin from other organisms and perhaps more importantly of site-directed mutants. This represents a substantial barrier to new structural and mechanistic studies.

Several groups[12−16] have previously purified wild-type or mutant αβ-tubulin from budding or fission yeast, however. These studies provided inspiration for our work by establishing the feasibility and potential of in vitro studies of fungal tubulins, and they also provided unique insights into the relationship between GTPase activity and MT dynamics,[13,17,18] into the role of isotype composition in determining MT dynamics,[19] and into the molecular determinants of interactions of αβ-tubulin with microtubule-associated proteins and with drugs.[16,20,21] Despite considerable promise, however, the methods used to date suffer from two significant limitations. First, the scope of expressible mutants is limited because these methods mostly express the mutant αβ-tubulins constitutively from the endogenous loci, and the mutants must therefore be able to functionally replace wild-type αβ-tubulin (see ref 16 for an exception). Second, the final yields of purified protein are relatively poor: these methods did not take advantage of maximal overexpression, because constitutive overexpression of αβ-tubulin is lethal in yeast.[22]

To improve the prospects for new structural and functional studies of αβ-tubulin, we wanted to create, overexpress, and purify

**Received:** April 6, 2011
**Revised:** July 29, 2011
**Published:** September 2, 2011

"nonpolymerizable" $\alpha\beta$-tubulin mutants with a blocked polymerization interface. Here, we report the design, overexpression, purification, and characterization of multiple polymerization-blocked mutants of yeast $\alpha\beta$-tubulin. To the best of our knowledge, these polymerization-blocked $\alpha\beta$-tubulin mutants are the first of their kind.

## EXPERIMENTAL PROCEDURES

**Plasmids and Strains.** To obtain plasmids capable of overexpressing tubulins, we amplified via polymerase chain reaction genes encoding Tub1p ($\alpha$-tubulin) and Tub2p ($\beta$-tubulin) for insertion into the inducible expression plasmids p426Gal1 and p424Gal1,[23] respectively (these are 2 $\mu$m plasmids that can be strongly induced when galactose is used as a carbon source). For template DNA, we used open reading frames ordered from Open Biosystems. The primers used to amplify Tub1 were 5′-GGCGGCGGATCCAAAATGAGAGAAGTTATTAGTATT-3′ (forward) and 5′-CGGCGGCTCGAGTTAAAATTCCTCTTCCTCAGCGTA-3′ (reverse); primers used to amplify Tub2 and append a C-terminal $His_6$ tag were 5′-GGCGGCCCCGGGAAAATGAGAGAAATCATTCATATC-3′ (forward) and 5′-CGGCGGCTGCAGTTAGTGGTGGTGGTGGTGGTGTTCAAAATTCTCAGTGATTGG-3′ (reverse). Underlined sequences highlight the restriction sites used for cloning: BamHI and XhoI for Tub1 and SmaI and PstI for Tub2. Mutant genes were prepared from these expression plasmids using QuikChange mutagenesis (Stratagene), following the manufacturer's instructions. Weakly inducible expression plasmids expressing wild-type or mutant tubulins were constructed by subcloning the appropriate coding region into p416GalS (for Tub1 constructs) or p415GalS (for Tub2 constructs);[23] these plasmids give substantially lower levels of maximal expression because they are maintained at close to single copy and they also carry a debilitated version of the Gal1 promoter. To obtain a plasmid capable of overexpressing the TOG1 domain (residues 1−317) from Stu2, we amplified this sequence from an open reading frame (Open Biosystems) using primers 5′-GGGCCCCCATGGGCTCAGGAGAAGAAGAAGTA-3′ (forward, NcoI) and 5′-CGCGCGCTGAGTCTAGTGGTGGTGGTGGTGGTGACTGAAGGTGTCTATTTGAAC-3′ (reverse, $His_6$, XhoI) and cloned it into pET15b (Novagen). To obtain a plasmid capable of overexpressing the *Schizosaccharomyces pombe* Eb1 homologue Mal3, we amplified this gene from *S. pombe* cDNA (a generous gift from S. Braun, University of California, San Francisco, CA) using primers 5′-GGGCCCCATATGGGCAGCCATCATCATCATCACAGCATGTCTGAATCTCGGCAAGAGC-3′ (forward, NdeI) and 5′-GCGCGCCTCGAGTTAAAACGTGATATTCTCATCGTC-3′ (reverse, XhoI) and cloned it into pET29b (Novagen). For all cloning, *Escherichia coli* strain DH5$\alpha$ was the host for DNA manipulation. The integrity of expression constructs was verified by sequencing performed by the McDermott Sequencing Core at the University of Texas Southwestern Medical Center.

**Protein Expression and Purification.** For strong overexpression of wild-type or mutant $\alpha\beta$-tubulin in yeast, the appropriate p426Gal1 and p424Gal1 plasmids were cotransformed into strain JEL1 (MAT$\alpha$ *leu2 trp1 ura3−52 prb1−1122 pep4−3 Δhis3::PGAL10-GAL4*).[24] Starting with small overnight cultures, we grew strains in 1 L of selective medium (CSM-Ura-Trp). This culture was then used to inoculate ∼15 L of YPGL (2% peptone, 1% yeast extract, 3% glycerol, and 2% lactate) in a homemade fermentation device that consisted of an autoclavable 20 L plastic carboy (Nalgene), a silicone barrel warmer (McMaster-Carr), and vigorous aeration to maintain cells in suspension. After approximately 24 h, galactose powder was added to 2%, and cells were induced for 3−5 h before being harvested. Cell pellets were frozen at −80 °C after being harvested. Using this base protocol, we typically obtained ∼100 g of cells (wet paste) from 15 L of culture. For protein purification, cell pellets were thawed and resuspended in lysis buffer [50 mM HEPES (pH 7.4), 500 mM NaCl, 10 mM $MgSO_4$, and 30 mM imidazole] with 1 mM PMSF before being ruptured by three passes through a microfluidizer (M110-P, Microfluidics) at ∼25000 psi. All purification steps were performed at 4 °C. The crude lysate was clarified by centrifugation (30 min at 17000*g* in an SS-34 rotor) before being loaded onto a 5 mL cartridge Ni-affinity column (Ni-NTA Superflow, Qiagen). After being extensively washed in lysis buffer and then low-salt buffer [25 mM HEPES (pH 7.4), 1 mM $MgSO_4$, and 30 mM imidazole], protein was eluted with elution buffer [25 mM PIPES (pH 6.9), 1 mM $MgSO_4$, and 250 mM imidazole]. Protein-containing fractions (identified using a Bradford assay) were pooled. Our estimate is that these pooled fractions are approximately one-third $\alpha\beta$-tubulin. At this point, the pooled eluate can by frozen after addition of glycerol to a final concentration of 20% or loaded directly onto a 2 mL Source-Q column (GE) and eluted with a 40 column volume NaCl gradient [buffer A being 25 mM PIPES (pH 6.9), 2 mM $MgSO_4$, 1 mM EGTA, and 50 $\mu$M GTP; buffer B being buffer A and 1 M NaCl]. The $\alpha\beta$-tubulin-containing fractions were pooled and dialyzed against buffer A before they were used. They can be frozen in liquid nitrogen and stored at −80 °C. The TOG1 domain from Stu2p (residues 1−317) and *S. pombe* Eb1 family member Mal3 were purified as described in refs 14, 25, and 26 with minor modifications.

**Phenotypic Assay.** For examining the effects of low-level expression of additional wild-type or mutant $\alpha\beta$-tubulin, the appropriate p416GalS and p415GalS plasmids were transformed into strain BY4742 (MATa his3Δ1 leu2Δ0 lys2Δ0 ura3Δ0).[27] We validated the assay by cloning "benchmark" mutants with known phenotype to serve as controls (see Results for details). Strains containing these benchmark mutants and/or candidate polymerization-blocked mutants were cultured in selective medium (CSM-URA-LEU for strains coexpressing Tub1 and wild-type or mutant Tub2, or CSM-URA for strains expressing only wild-type or mutant Tub1). Serial 10-fold dilutions of cultures were transferred to selective plates containing 2% glucose (noninducing) or 2% galactose (inducing) using an inoculating manifold and imaged after being grown for 3−4 days at 30 °C. To identify a growth phenotype from the Tub1 mutants, it was necessary to add a variable amount of the microtubule stress agent benomyl to the plates (in the range of 5−15 $\mu$g/mL).

**In Vitro Assays.** Gel filtration experiments were performed by loading 200 $\mu$L of 5 $\mu$M protein onto a Superdex 200 10/300 column equilibrated in 25 mM Tris (pH 7.5), 200 mM NaCl, 1 mM $MgCl_2$, and 1 mM EGTA. The bed volume of the column is 25 mL, and the void volume is 8.2 mL. GTP binding experiments were performed using a filter binding assay adapted from ref 28. Briefly, 0.5 $\mu$M $\alpha\beta$-tubulin samples were incubated in binding buffer [25 mM PIPES (pH 6.9), 1 mM EGTA, 2 mM $MgCl_2$, 50 $\mu$g/mL BSA, 5 $\mu$M GTP, and 100 $\mu$M ATP] containing [$\gamma$-$^{32}$P]GTP, applied to BA85 nitrocellulose filters, and rapidly washed with wash buffer [25 mM PIPES (pH 6.9), 2 mM $MgCl_2$, and 1 mM EGTA]. Radioactivity was measured by scintillation counting. Experiments were performed in quadruplicate, and results were corrected for

background by subtracting the counts measured from reaction mixtures that did not contain $\alpha\beta$-tubulin. Microtubule "spin-down" experiments for assaying polymerization were performed by incubating protein in assembly buffer [2.5−10% glycerol, 100 mM PIPES (pH 6.9), 2 mM $MgSO_4$, and 0.20 mM EGTA] for 30 min at 30 °C. For electrophoretic analysis, the contents of the assembly reaction mixtures were spun at 96000*g* at 30 °C for 30 min in a prewarmed TLA-100 rotor, the supernatant was carefully removed, and the pellet was resuspended in 1× SDS buffer such that pellet and supernatant fractions had equal volumes. For fluorescence imaging, a portion of the assembly reaction mixture was cross-linked by 10-fold dilution into assembly buffer containing 1% glutaraldehyde. Cross-linking was quenched by 5-fold dilution into assembly buffer containing 20 mM Tris (pH 6.9), and 30 $\mu$L of these quenched, cross-linked reaction mixtures was then applied to the top of a glycerol cushion [20% glycerol in BRB80, BRB80 being 80 mM PIPES (pH 6.8), 1 mM $MgCl_2$, and 1 mM EGTA] and spun through the cushion onto polylysine-coated coverslips. Coverslips were stained using FITC-DM1$\alpha$ (Sigma-Aldrich) for imaging by fluorescence. The experiments for determining the critical concentration for polymerization were performed similarly, with the following modifications: the incubation time was 45 min, and no cross-linking was performed. $\alpha\beta$-Tubulin concentrations in the supernatant and pellet were quantified by the Bradford assay. Circular dichroism (CD) experiments were performed after protein had been exchanged into 20 mM sodium phosphate, 5 mM $MgSO_4$, and 0.1 mM GTP (pH 7.0). CD spectra were recorded at room temperature using an AVIV 62DS spectrometer. Data were collected with 1 nm spacing, using 3s averaging at each point. Three scans were averaged to yield the data shown. After a buffer scan had been subtracted, spectra were normalized to units of mean molar residue ellipticity (degrees square centimeter per decimole per residue) using protein concentrations determined by amino acid analysis (performed by the Keck Biotechnology Resource Laboratory at Yale University, New Haven, CT) according to the equation $[\theta(\lambda)] = \theta_{obs}(\lambda)/(10ncl)$, where $[\theta(\lambda)]$ is the mean residue molar ellipticity as a function of wavelength, $n$ is the number of residues in the protein, $c$ is the concentration of the protein (molar), $l$ is the sample path length (centimeters), and $\theta_{obs}(\lambda)$ is the observed ellipticity as a function of wavelength (nanometers).

## RESULTS

**Purification of $\alpha\beta$-Tubulin from Overexpressing Strains of Yeast.** We cloned Tub1 and Tub2 into inducible expression plasmids, cotransformed these plasmids into yeast, and induced expression in densely growing yeast cultures. Western blots clearly demonstrate inducible overexpression of both Tub1p and Tub2p (Figure 1A) in strains carrying the tubulin overexpression plasmids we constructed. Using a relatively simple two-step purification, we obtain multimilligram quantities of very pure Tub1p:Tub2p-$H_6$ (~3−4 mg from 100 g of cells) (Figure 1). These yields are approximately 4-fold higher than those reported previously,[15,20] a modest gain that nevertheless has significant practical benefits because it reduces the cumbersome work associated with large culture volumes. For example, 100 g of cell paste can be obtained from as little as 1 L of culture using fed batch fermentation (data not shown). We performed several experiments to demonstrate that the purified yeast $\alpha\beta$-tubulin was functional. First, the tubulin is purified as a stoichiometric heterodimer (see the lightly loaded lane in Figure 1B where distinct bands are visible for Tub1p and Tub2p) even though only Tub2p carries a $His_6$ tag. Second, the purified $\alpha\beta$-tubulin readily forms MTs (Figure 1C) that assemble with a critical concentration of ~1 $\mu$M as judged by linear extrapolation of pelleting material (Figure 1D), consistent with prior observations.[13] Third, the purified $\alpha\beta$-tubulin shows an elution profile virtually identical to that of animal $\alpha\beta$-tubulin on a gel filtration column (Figure 2A) (both elute at 13.6 mL from a Superdex 200 10/300 column with a bed volume of 25 mL and a void volume of 8.2 mL), indicating that the yeast $\alpha\beta$-tubulin is free of aggregation defects and has the expected hydrodynamic properties. Fourth, we confirmed two known interactions with regulatory proteins, showing that the purified $\alpha\beta$-tubulin forms a complex with the TOG1 domain from Stu2p (recapitulating results of refs 25 and 26 but using yeast $\alpha\beta$-tubulin) (Figure 2B), and that it is stimulated to polymerize by the addition of the Eb1 family protein Mal3 (observing much more numerous, shorter microtubules in the presence of Mal3 recapitulates results of ref 14 showing that Mal3 stimulates MT assembly) (Figure 2C). The Mal3-dependent stimulation of assembly can also be readily observed by sodium dodecyl sulfate−polyacrylamide gel electrophoresis (SDS−PAGE) analysis of spindowns (data not shown). Finally, we used a filter binding assay to demonstrate that at equal concentrations, the purified $\alpha\beta$-tubulin binds an amount of

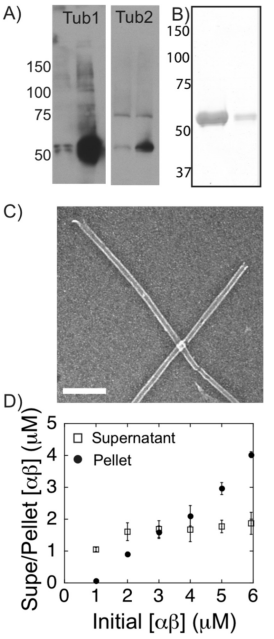


**Figure 1.** Overexpression and purification of yeast $\alpha\beta$-tubulin with assays for its polymerization properties. (A) Western blots before (left) and after (right) induction with galactose demonstrate significant overexpression of both Tub1p and Tub2p (loading was normalized by the $A_{600}$ of the culture). (B) SDS−PAGE of the purified $\alpha\beta$-tubulin, with one heavily loaded (5.1 $\mu$g) lane to demonstrate purity and one lightly loaded (0.2 $\mu$g) lane to better resolve the closely spaced bands for Tub1p and Tub2p. (C) Negative stain electron micrograph demonstrating that the purified yeast $\alpha\beta$-tubulin forms MTs (bar is 200 nm) (right). (D) Protein concentrations in the supernatant (□) and pellet (●) fractions of microtubule assembly reaction mixtures plotted as a function of the initial $\alpha\beta$-tubulin concentration. Error bars indicate the standard deviation of three independent measurements. The critical concentration for assembly is 0.95 $\mu$M as measured by linear extrapolation of pelleted material to $y = 0$ and 1.75 $\mu$M as measured by the constant amount of material in the supernatant.


dx.doi.org/10.1021/bi2005174 | *Biochemistry* 2011, 50, 8636−8644

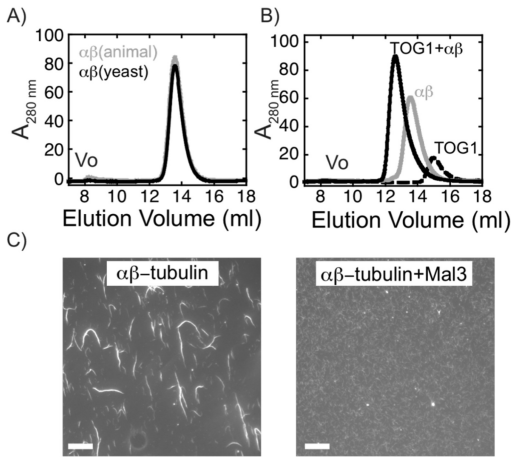


**Figure 2.** Purified yeast $\alpha\beta$-tubulin shows the expected hydrodynamic properties and interacts normally with two different $\alpha\beta$-tubulin binding proteins. (A) Comparative gel filtration chromatography showing that yeast (black) and animal brain (gray) $\alpha\beta$-tubulin elute at almost identical volumes (13.6 mL on a Superdex 200 10/300 column), consistent with the 100 kDa molecular mass of an $\alpha\beta$-tubulin heterodimer. (B) Gel filtration chromatography showing that the purified yeast $\alpha\beta$-tubulin (gray) forms a complex (black) with the TOG1 domain from Stu2p (black dashed). (C) Fluorescence micrographs demonstrating that the purified yeast $\alpha\beta$-tubulin is stimulated to form MTs by the addition of Eb1 family protein Mal3 (bar is 25 $\mu$m).

GTP similar to that bound by animal $\alpha\beta$-tubulin (see Figure 6). The observed binding is specific because it can be competed away with excess cold GTP, occurs in the presence of excess cold ATP, and depends on the concentration of $\alpha\beta$-tubulin present in the reaction mixtures. We also verified that the microtubule-stabilizing drug epothilone enhanced the polymerization of purified $\alpha\beta$-tubulin (as demonstrated in ref 29; see Figure 5). Together, these data indicate that the $\alpha\beta$-tubulin purified from overexpressing strains is functional.

**A Phenotypic Assay for Inducible Dominant Negative Phenotypes.** We hypothesized that mutants with a blocked polymerization interface would inhibit polymerization by reversibly capping protofilaments, and that they should therefore give a dominant-negative phenotype when expressed in yeast. If true, this would provide a convenient assay for rapidly ranking the order of potency of candidate mutants. To explore this possibility, we first developed and validated a plate assay (Figure 3) to screen for an inducible dominant-negative phenotype using galactose-inducible plasmids to express viable and dominant negative alleles of $\alpha\beta$-tubulin that had been previously identified by genetic screening (dominant lethal mutants include Tub1-E255A[30] and Tub2-E327A,D328A,E329A, which was previously described as Tub2−446;[31] benign mutants include Tub1p-R327A,D328A,R331A and Tub2p-E125A,D128A, previously described as Tub1−835[32] and Tub2−422,[31], respectively). We were able to avoid the toxicity associated with overexpression of wild-type $\alpha\beta$-tubulin[22] by taking advantage of expression plasmids that give very low maximal expression levels[23] (see Experimental Procedures). Tub2p-expressing plasmids were always balanced by a plasmid expressing wild-type Tub1 to avoid the toxicity of unbalanced Tub2p expression.[22] Overexpression of Tub1p in yeast is not nearly as deleterious, so cotransforming a plasmid expressing Tub2 was not necessary. In this assay, inducing the expression of the known dominant-negative $\alpha\beta$-tubulin mutants (listed above) strongly inhibited cell growth, but inducing expression of wild-type or "neutral" alleles (listed above) was without significant consequences (Figure 3).

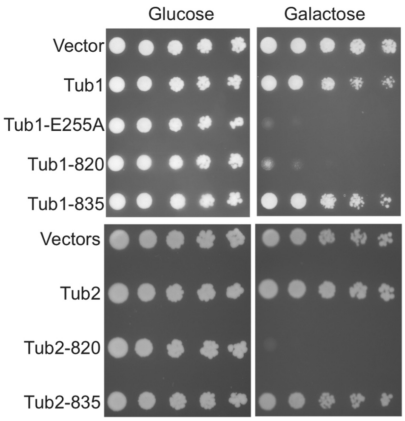


**Figure 3.** Phenotypic assay for an inducible dominant-negative growth defect validated using mutant $\alpha$- or $\beta$-tubulin alleles of known phenotype. Strains expressing wild-type and/or previously characterized benign (Tub1−835 and Tub2−422) and dominant lethal (Tub1-E255A, Tub1−820, and Tub2−446) alleles (see Experimental Procedures) of Tub1 or Tub2 from galactose-inducible plasmids were plated onto glucose (noninducing) or galactose (inducing plates). Expressing known dominant lethal alleles identified in previous alanine scanning experiments[30−32] gives a strong inducible growth phenotype, but expressing wild-type or benign alleles does not.

**Design and Phenotypic Characterization of Polymerization-Blocking Mutants.** The tendency of $\alpha\beta$-tubulin to polymerize represents a significant obstacle to structural and biochemical studies. A key feature of our overexpression strategy is that it should expand the scope of "purifiable" mutants by eliminating the requirement that the mutants support viability. In what follows, we explore this in more detail by demonstrating that it is possible to overexpress and purify site-directed and dominant lethal mutant forms of $\alpha\beta$-tubulin that cannot polymerize because the mutations "blocked" a polymerization interface. A similar approach has been used successfully to create a nonpolymerizable actin mutant[33] that has led to multiple new structures of actin.[34−36] To the best of our knowledge, no analogous tubulin mutants exist.

For practical reasons, we initially targeted the longitudinal interface: it is thought to be significantly stronger than the lateral interface, and it has been defined in atomic detail[5,37−39](also see Figure 3). Guided by the structure of $\alpha\beta$-tubulin,[5,6] we introduced several sets of mutations on the plus (Tub2p) or minus (Tub1p) end surfaces of the heterodimer that we predicted would interfere with longitudinal interactions without otherwise compromising the structural integrity of the protein (Figure 4). We chose residues to mutate by manually identifying interfacial side chains with substantial solvent exposure in the isolated $\alpha\beta$-tubulin heterodimer but that become buried by longitudinal association. We introduced disruptive mutations by altering the charge and/or size of the chosen residues. We introduced a number of mutations on either the plus or minus end of $\alpha\beta$-tubulin (Figure 4, Table 1, and data not shown).

We then used our phenotypic plate assay to screen candidate blocked mutants for their ability to produce an inducible dominant-negative growth phenotype. Inducing the expression of the candidate-blocked $\beta$-tubulin (Tub2p) mutants gave very strong growth inhibition (Figure 4). This result is consistent with the idea that the mutants were poisoning normal microtubule


dx.doi.org/10.1021/bi2005174|Biochemistry 2011, 50, 8636−8644

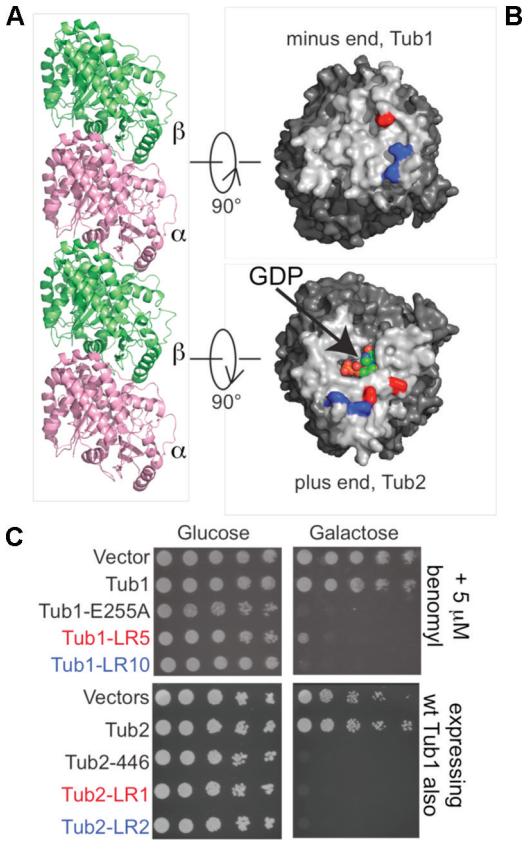


**Figure 4.** Design and phenotypic characterization of mutations to block each of two polymerization interfaces of $\alpha\beta$-tubulin. (A) Representation of the longitudinal association between two $\alpha\beta$-tubulin ($\alpha$, pink; $\beta$, green) as revealed in the crystal structure of the "straight" conformation of $\alpha\beta$-tubulin.[5] (B) Surface views of the plus (bottom) and minus (top) end of the interacting $\alpha\beta$-tubulin heterodimers. The surface area buried by the association is depicted in a lighter color, and the nucleotide bound to $\beta$-tubulin is represented as spheres. The locations of candidate blocking mutations on the longitudinal interface of Tub1 and Tub2 are colored blue or red, and the amino acid changes are listed in Table 1. (C) Expressing the blocked mutants in yeast produces a strong dominant-negative phenotype, whereas expressing wild-type tubulins does not. Tub2−446 and Tub1-E255A are known dominant lethal alleles that were used as positive controls (see Figure 2). For the Tub1 experiment only, the plates contain 5 $\mu$g/mL benomyl; for the Tub2 experiments, all strains (except empty vectors) also inducibly express wild-type Tub1 to avoid the deleterious effects of unbalanced Tub2 expression.

**Table 1. Interface-Blocking Mutations on Tub1p ($\alpha$-tubulin) and Tub2p ($\beta$-tubulin)[a]**

| | |
|---|---|
| Tub1-LR5 | T349E |
| Tub1-LR10 | T326Q,Q330W |
| Tub2-LR1 | T175R,V179R |
| Tub2-LR2 | F394A,W397E |

[a]Polymerization-blocked mutants on the minus end (Tub1) and plus end (Tub2) of yeast $\alpha\beta$-tubulin.

behavior by interfering with subunit addition at the plus end of microtubules.

Initially, we were surprised to note that inducing expression of all candidate-blocked $\alpha$-tubulin (Tub1p) mutants failed to produce significant growth defects (data not shown). This is in marked contrast to the strong dominant lethal phenotype of Tub1p-E255A and Tub1p-820 (Figure 4) and to the results obtained with candidate-blocked Tub2 mutants (Figure 4). We reasoned that because plus end growth is the dominant mode of MT growth in yeast,[40] a heterodimer blocked on its minus end might effectively be "invisible" to the growing polymer. This could explain the apparent lack of growth phenotype, because the primary effect of expressing such a mutant at low levels would essentially be an only slight "dilution" of the amount of functional $\alpha\beta$-tubulin. We hypothesized that the effects of such a mutant might become more readily apparent under conditions of microtubule stress. Rescreening of the mutants in the presence of increasing concentrations of a microtubule stress agent, benomyl, revealed substantial dominant-negative growth phenotypes for several of our designed minus end mutants (Figure 4 and Table 1). These results are consistent with (but do not unambiguously establish) a blocking effect of the plus end and minus end mutations. Ongoing work in our laboratory is examining how expression of these plus and minus end-blocked mutant $\alpha\beta$-tubulins affects the microtubule cytoskeleton in vivo (not shown).

**Purification and in Vitro Characterization of $\alpha\beta$-Tubulin Mutants Blocked on the Plus or Minus End.** To directly probe the polymerization behavior of candidate-blocked mutants outside the cell, and to rule out the possibility that the mutant-induced growth defect resulted from folding or other defects unrelated to polymerization, we overexpressed and purified a number of mutants for in vitro studies. We prepared strains carrying the mutant genes on strong galactose-inducible expression plasmids (see Experimental Procedures), and we grew and induced these strains as described above for wild-type $\alpha\beta$-tubulin. Using the same purification protocol, we purified milligram amounts of candidate polymerization-blocked mutants. The mutants we chose to pursue in vitro all gave strong inducible growth defects in the phenotypic assay, so their purification demonstrates that it is possible to purify biochemically relevant quantities of otherwise lethal $\alpha\beta$-tubulin mutants (see refs 16 and 21 for recent examples of purifying lethal mutations, albeit at substantially lower yields). In what follows, we will focus on more detailed in vitro characterization of two strongly blocked mutants, one on each longitudinal surface of the heterodimer.

We analyzed the polymerization behavior of the mutants using a bulk assay for microtubule assembly. $\alpha\beta$-Tubulins were incubated under microtubule assembly conditions, and polymerized and unpolymerized $\alpha\beta$-tubulins were separated by centrifugation. The extent of polymerization was assessed by Coomassie gel analysis of the supernatant and pellet and verified by microscopic examination of the polymerization reactions. These experiments revealed that the blocked mutants are severely compromised for self-assembly. Under conditions where wild-type $\alpha\beta$-tubulin readily forms microtubules, the plus and minus end-blocked mutants do not (Figure 5A and data not shown). Even when challenged with epothilone, a natural product that drives polymerization by stabilizing microtubules, the mutants fail to polymerize (Figure 5A). This resistance to epothilone-induced polymerization cannot be trivially explained by a defect in epothilone binding, because the sites of mutation are distant from the epothilone-binding site (which is near a lateral interface[41]). We also examined how variable doses of plus end or minus end-blocked mutants affected the polymerization of wild-type tubulin when present in a mixture. At stoichiometries of 1:1 and lower, the presence of either blocked mutant potently inhibited the ability of wild-type tubulin to


dx.doi.org/10.1021/bi2005174 | Biochemistry 2011, 50, 8636–8644

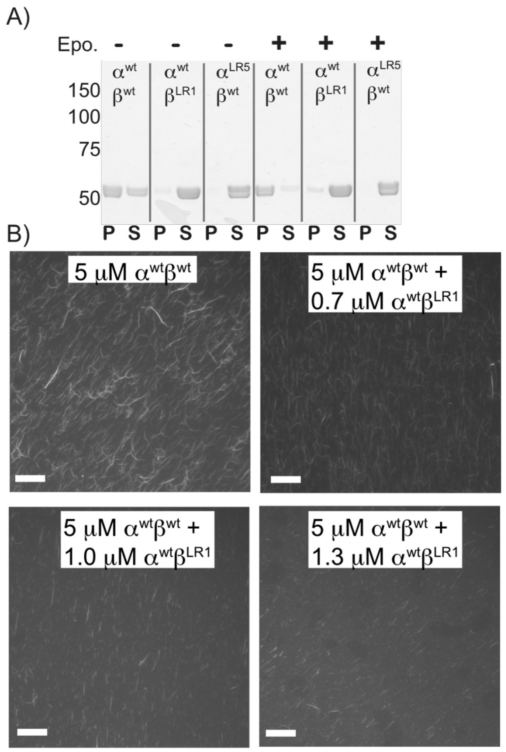


**Figure 5.** Purified $\alpha\beta$-tubulin mutants have a severe polymerization defect. (A) SDS–PAGE analysis of spindown experiments (P, pellet; S, supernatant) demonstrates that tubulins with blocking mutations on the plus (Tub2) or minus (Tub1) end of the heterodimer do not self-assemble under conditions where wild-type $\alpha\beta$-tubulin readily forms MTs. The polymerization defect is severe, because the mutants resist the action of epothilone, a natural product that drives MT assembly because it stabilizes MTs. (B) Fluorescence micrographs of MT assembly reaction mixtures containing identical concentrations (5 $\mu$M) of wild-type $\alpha\beta$-tubulin but with variable amounts of the mutant heterodimer containing the blocked Tub2-LR1 (top left, no mutant; top right, 10% blocked mutant; bottom left, 15% blocked mutant; bottom right, 20% blocked mutant) show that the blocked mutant interferes with the assembly of wild-type $\alpha\beta$-tubulin at stoichiometries as low as ~1:7. Presumably, this inhibition occurs because the mutant binds to and poisons the growth of microtubules and/or microtubule assembly intermediates (bar is 25 $\mu$m).

form microtubules (Figure 5B). Thus, even under conditions where the concentration of wild-type $\alpha\beta$-tubulin present would ordinarily be sufficient to form abundant microtubules, the presence of a blocked mutant is strongly inhibitory. Presumably, this "in vitro dominant-negative" behavior results because the mutants use their "normal" polymerization interfaces to bind to microtubule initiation intermediates and/or to elongating microtubules, and this binding poisons growth because the blocked interface interferes with further subunit addition. In the bulk assays, we observe significant inhibition of assembly down to mutant:wild-type stoichiometries as low as 1:6 [~17% (Figure 5B)].

Biochemical characterization indicates that the mutations do not compromise the folding and polymerization-independent properties of the heterodimers. Indeed, like the wild-type protein, they are purified as heterodimers that migrate normally on gel filtration (Figure 6). They also remain competent to bind GTP as determined by a filter binding assay (Figure 6). Finally, the mutants retain the ability to bind the TOG1 domain from Stu2p in a gel filtration assay. We were unable to test interactions with Mal3, as we did for wild-type $\alpha\beta$-tubulin, because these interactions require MT formation. However, consistent with the indirect assays for structural integrity described above, wild-type and plus end-blocked mutants give very similar circular dichroism spectra (Figure 6). Together, these observations suggest that the biochemical consequences of mutations introduced on the polymerization interfaces are local, without significant consequences for the biochemical properties of distant sites (Figure 6).

## DISCUSSION

The near exclusive use of animal brain $\alpha\beta$-tubulin represents a significant obstacle to in vitro studies of $\alpha\beta$-tubulin structure and biochemistry. One reason for this is the fact that $\alpha\beta$-tubulin purified from animal brains is a mixture of multiple $\alpha$- and $\beta$-tubulin isotypes. This isotypic heterogeneity complicates mechanistic analysis: the different isotypes can have different biochemical properties, but experimental observations represent population-weighted averages. Interpreting measurements taken in the presence of heterogeneity with a single set of parameters that ignores these differences may not always be appropriate. Furthermore, and for obvious reasons, animal brain $\alpha\beta$-tubulin cannot be subjected to powerful and ordinarily routine techniques like site-directed mutagenesis. As a result, only a small handful of studies[15−18,20,21] have attempted to use surface mutagenesis of $\alpha\beta$-tubulin to modulate the interactions of $\alpha\beta$-tubulin with itself and/or to map or modulate the interactions of $\alpha\beta$-tubulin with regulatory factors. To address these and other limitations, we sought to develop a new source of recombinant $\alpha\beta$-tubulin that would be amenable to site-directed mutagenesis.

We first described techniques that allow affinity-tagged wild-type yeast $\alpha\beta$-tubulin to be purified from inducibly overexpressing strains of yeast. We chose yeast as an expression host because stringent requirements for eukaryote-specific chaperones have so far prevented the expression of functional $\alpha\beta$-tubulin in bacteria, and methods for purifying fungal $\alpha\beta$-tubulins from yeast already existed.[12−16] Yeast and animal $\alpha\beta$-tubulin form microtubules with different dynamic properties, so systematically studying the polymerization dynamics of this non-animal $\alpha\beta$-tubulin should provide new mechanistic insight into the biochemical determinants of microtubule dynamics. However, because the constitutive overexpression of $\alpha\beta$-tubulin is lethal in yeast,[22] obtaining fungal $\alpha\beta$-tubulins in sufficient quantities using already existing methods was cumbersome and challenging. By avoiding the limitations associated with constitutive expression from the genomic loci, inducible overexpression increased yields by at least 4-fold over the best yields previously reported.[20] The purified $\alpha\beta$-tubulin passes multiple tests for function: it polymerizes with a critical concentration consistent with prior studies,[13] binds GTP, and interacts with the two regulatory proteins that we tested. The milligram-scale yields we obtain remain admittedly low compared to what can be achieved with animal brains (~50 mg up to grams depending on the number of brains used), but as discussed below, we believe that this disadvantage is significantly outweighed by the potential benefits that will accompany routine access to site-directed $\alpha\beta$-tubulin mutants.

To establish that inducible overexpression of $\alpha\beta$-tubulin in yeast represented a general strategy for purifying wild-type or mutant $\alpha\beta$-tubulin, we wanted to purify a mutant that could not support viability using the same protocol developed to purify wild-type $\alpha\beta$-tubulin. Depending on the mutant, this expression and purification would be difficult if not impossible using the preexisting methods for purifying fungal $\alpha\beta$-tubulin, because

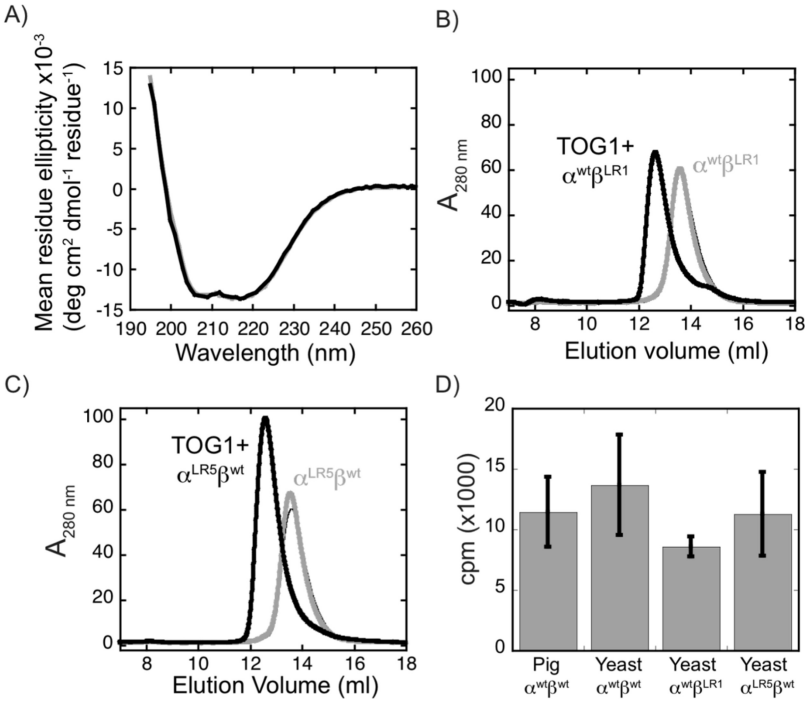


**Figure 6.** Polymerization-blocked mutants of $\alpha$- and $\beta$-tubulin do not have gross structural defects and appear normal by other biochemical measures. (A) Circular dichroism spectra for the wild type (gray) and the plus end-blocked mutant (black) are very similar. (B and C) Mutants with blocking mutations on the plus end (B) or on the minus end (C) migrate normally on gel filtration (gray curves; the thin black curve shows the elution profile of wild-type $\alpha\beta$-tubulin for reference) and remain competent to interact with the TOG1 domain from Stu2p (black curves). (D) A filter binding assay demonstrates that at equal concentrations, blocked mutants of Tub1 or Tub2 bind comparable amounts of GTP like wild-type yeast or porcine $\alpha\beta$-tubulin does.

constitutive expression of a nonviable $\alpha\beta$-tubulin mutant would be lethal.

Prior genetic studies have identified a number of lethal mutant $\alpha\beta$-tubulin alleles in yeast, but purifying one of them for the kind of proof-of-principle experiments described here did not seem optimal: because the mechanistic effect of the mutation-induced changes for many of these alleles has not yet been determined, showing that the in vitro behavior of the mutant was consistent with its in vivo phenotype would not have been straightforward. Instead of using a preexisting allele, and also because we have an interest in facilitating new structural studies of $\alpha\beta$-tubulin, we instead chose to design and purify the first polymerization-blocked lethal alleles of $\alpha\beta$-tubulin as a way to demonstrate the robustness of our expression and purification strategy.

The tendency to polymerize makes $\alpha\beta$-tubulin notoriously difficult to crystallize. The very few structures of $\alpha\beta$-tubulin that are available (a conformation compatible with microtubule structure was determined using electron crystallography,[5,39] and a conformation incompatible with microtubule structure was determined by X-ray crystallography of a complex with a microtubule depolymerizing factor[6]) have framed our understanding in vital ways. However, despite intense effort, fundamental structural questions about $\alpha\beta$-tubulin conformation and about how microtubule-associated proteins recognize $\alpha\beta$-tubulin remain unanswered. New structures of $\alpha\beta$-tubulin will be required to resolve these and other long-standing issues. Inspired by an analogous approach that produced nonpolymerizable actin mutants,[33] we took advantage of the existing structures of $\alpha\beta$-tubulin to design "polymerization-blocking" mutations on longitudinal self-association interfaces. Our approach targeted solvent-exposed sites on the longitudinal polymerization interfaces that become substantially buried by self-assembly contacts. We then introduced mutations that we anticipated would be very disruptive to polymerization, typically replacing small, uncharged side chains (e.g., $\alpha$-tubulin T349 or $\beta$-tubulin V179) with large, charged ones (e.g., $\alpha$-tubulin T349E or $\beta$-tubulin V179R). Our approach was not intended to be exhaustive, and it is likely that other sites and/or substitutions can also produce polymerization-blocked $\alpha\beta$-tubulins. However, because these first designs met our criteria (dominant lethal phenotype, inability to polymerize in vitro, and inhibitory activity against the polymerization of wild-type $\alpha\beta$-tubulin) for a severe polymerization block, we have begun to focus on the design and purification of other classes of mutants.

In summary, the results reported here represent a significant technical advance that overcomes several longstanding problems that had been associated with the widespread reliance on endogenous brain $\alpha\beta$-tubulin and/or purification of recombinant $\alpha\beta$-tubulin from sources constitutively expressing it. The blocked mutants we developed appear to behave as exquisitely specific competitive inhibitors of polymerization, and it therefore seems likely that using them in functional assays will provide new insights into the mechanisms underlying microtubule polymerization dynamics. On the structural front, we have already used the plus end-blocked mutant described here to determine a new structure of $\alpha\beta$-tubulin bound to a regulatory protein (to be reported elsewhere), and we anticipate that more structures will be forthcoming. More generally, because site-directed $\alpha\beta$-tubulin mutants can now be purified much more routinely, it should now be possible to purify any number of $\alpha\beta$-tubulin mutants identified in prior genetic screens, and by studying their behavior in vitro, we should gain deeper mechanistic insight into the biochemical changes underlying the mutant phenotype. Our preliminary experiments also suggest that it will be possible to purify yet other classes of mutants, including, for example, those incorporating

peptide tags for site-specific fluorescent labeling or with any number of other engineered modifications designed to facilitate new measurements or probe specific molecular features or interactions. These results establish robust methods for identifying and purifying mutant $\alpha\beta$-tubulins, including mutants that would otherwise be lethal. The mutants with blocked assembly interfaces that we developed represent unique reagents that open new experimental approaches and revitalize old ones.

## AUTHOR INFORMATION

### Corresponding Author

*E-mail: luke.rice@utsouthwestern.edu. Phone: (214) 645-5931. Fax: (214) 645-6387.

### Funding

This work was supported by funding from the Robert A. Welch Foundation (Grant I-1692) and the National Science Foundation (Grant MCB-1054947). L.M.R. is the Thomas O. Hicks Scholar in Medical Research.

## ACKNOWLEDGMENTS

We thank Na Wang for help with cloning and with protein expression and purification early in the project, Youxing Jiang and his lab for assistance with fermentation, Elliott Ross for assistance with the filter binding assay, and Sigurd Braun for a gift of *S. pombe* cDNA.

## ABBREVIATIONS

MT, microtubule; MAPs, microtubule-associated proteins.

## REFERENCES

(1) Desai, A., and Mitchison, T. J. (1997) Microtubule polymerization dynamics. *Annu. Rev. Cell Dev. Biol. 13*, 83−117.

(2) Horio, T., and Hotani, H. (1986) Visualization of the dynamic instability of individual microtubules by dark-field microscopy. *Nature 321*, 605−607.

(3) Mitchison, T., and Kirschner, M. (1984) Dynamic instability of microtubule growth. *Nature 312*, 237−242.

(4) Walker, R. A., O'Brien, E. T., Pryer, N. K., Soboeiro, M. F., Voter, W. A., Erickson, H. P., and Salmon, E. D. (1988) Dynamic instability of individual microtubules analyzed by video light microscopy: Rate constants and transition frequencies. *J. Cell Biol. 107*, 1437−1448.

(5) Löwe, J., Li, H., Downing, K. H., and Nogales, E. (2001) Refined structure of $\alpha\beta$-tubulin at 3.5 Å resolution. *J. Mol. Biol. 313*, 1045−1057.

(6) Ravelli, R. B. G., Gigant, B., Curmi, P. A., Jourdain, I., Lachkar, S., Sobel, A., and Knossow, M. (2004) Insight into tubulin regulation from a complex with colchicine and a stathmin-like domain. *Nature 428*, 198−202.

(7) Barbier, P., Dorleans, A., Devred, F., Sanz, L., Allegro, D., Alfonso, C., Knossow, M., Peyrot, V., and Andreu, J. M. (2010) Stathmin and interfacial microtubule inhibitors recognize a naturally curved conformation of tubulin dimers. *J. Biol. Chem. 285*, 31672−31681.

(8) Buey, R. M., Díaz, J. F., and Andreu, J. M. (2006) The nucleotide switch of tubulin and microtubule assembly: A polymerization-driven structural change. *Biochemistry 45*, 5933−5938.

(9) Rice, L. M., Montabana, E. A., and Agard, D. A. (2008) The lattice as allosteric effector: Structural studies of $\alpha\beta$- and $\gamma$-tubulin clarify the role of GTP in microtubule assembly. *Proc. Natl. Acad. Sci. U.S.A. 105*, 5378−5383.

(10) Wang, H.-W., and Nogales, E. (2005) Nucleotide-dependent bending flexibility of tubulin regulates microtubule assembly. *Nature 435*, 911−915.

(11) Nogales, E., and Wang, H.-W. (2006) Structural mechanisms underlying nucleotide-dependent self-assembly of tubulin and its relatives. *Curr. Opin. Struct. Biol. 16*, 221−229.

(12) Barnes, G., Louie, K. A., and Botstein, D. (1992) Yeast proteins associated with microtubules in vitro and in vivo. *Mol. Biol. Cell 3*, 29−47.

(13) Davis, A., Sage, C. R., Wilson, L., and Farrell, K. W. (1993) Purification and biochemical characterization of tubulin from the budding yeast *Saccharomyces cerevisiae*. *Biochemistry 32*, 8823−8835.

(14) des Georges, A., Katsuki, M., Drummond, D., Osei, M., Cross, R., and Amos, L. (2008) Mal3, the *Schizosaccharomyces pombe* homolog of EB1, changes the microtubule lattice. *Nat. Struct. Mol. Biol. 15*, 1102−1108.

(15) Gupta, M. L., Bode, C. J., Thrower, D. A., Pearson, C. G., Suprenant, K. A., Bloom, K. S., and Himes, R. H. (2002) $\beta$-Tubulin C354 mutations that severely decrease microtubule dynamics do not prevent nuclear migration in yeast. *Mol. Biol. Cell 13*, 2919−2932.

(16) Uchimura, S., Oguchi, Y., Katsuki, M., Usui, T., Osada, H., Nikawa, J.-i., Ishiwata, S. i., and Muto, E. (2006) Identification of a strong binding site for kinesin on the microtubule using mutant analysis of tubulin. *EMBO J. 25*, 5932−5941.

(17) Davis, A., Sage, C. R., Dougherty, C. A., and Farrell, K. W. (1994) Microtubule dynamics modulated by guanosine triphosphate hydrolysis activity of $\beta$-tubulin. *Science 264*, 839−842.

(18) Dougherty, C. A., Sage, C. R., Davis, A., and Farrell, K. W. (2001) Mutation in the $\beta$-tubulin signature motif suppresses microtubule GTPase activity and dynamics, and slows mitosis. *Biochemistry 40*, 15725−15732.

(19) Bode, C. J., Gupta, M. L., Suprenant, K. A., and Himes, R. H. (2003) The two $\alpha$-tubulin isotypes in budding yeast have opposing effects on microtubule dynamics in vitro. *EMBO Rep. 4*, 94−99.

(20) Gupta, M. L., Bode, C. J., Georg, G. I., and Himes, R. H. (2003) Understanding tubulin-Taxol interactions: Mutations that impart Taxol binding to yeast tubulin. *Proc. Natl. Acad. Sci. U.S.A. 100*, 6394−6397.

(21) Uchimura, S., Oguchi, Y., Hachikubo, Y., Ishiwata, S. i., and Muto, E. (2010) Key residues on microtubule responsible for activation of kinesin ATPase. *EMBO J. 29*, 1167−1175.

(22) Burke, D., Gasdaska, P., and Hartwell, L. (1989) Dominant effects of tubulin overexpression in *Saccharomyces cerevisiae*. *Mol. Cell. Biol. 9*, 1049−1059.

(23) Mumberg, D., Müller, R., and Funk, M. (1994) Regulatable promoters of *Saccharomyces cerevisiae*: Comparison of transcriptional activity and their use for heterologous expression. *Nucleic Acids Res. 22*, 5767−5768.

(24) Lindsley, J. E., and Wang, J. C. (1993) On the coupling between ATP usage and DNA transport by yeast DNA topoisomerase II. *J. Biol. Chem. 268*, 8096−8104.

(25) Al-Bassam, J., van Breugel, M., Harrison, S. C., and Hyman, A. (2006) Stu2p binds tubulin and undergoes an open-to-closed conformational change. *J. Cell Biol. 172*, 1009−1022.

(26) Slep, K. C., and Vale, R. D. (2007) Structural Basis of Microtubule Plus End Tracking by XMAP215, CLIP-170, and EB1. *Mol. Cell 27*, 976−991.

(27) Brachmann, C. B., Davies, A., Cost, G. J., Caputo, E., Li, J., Hieter, P., and Boeke, J. D. (1998) Designer deletion strains derived from *Saccharomyces cerevisiae* S288C: A useful set of strains and plasmids for PCR-mediated gene disruption and other applications. *Yeast 14*, 115−132.

(28) Brandt, D. R., and Ross, E. M. (1986) Catecholamine-stimulated GTPase cycle. Multiple sites of regulation by $\beta$-adrenergic receptor and $Mg^{2+}$ studied in reconstituted receptor-Gs vesicles. *J. Biol. Chem. 261*, 1656−1664.

(29) Bode, C., Gupta, M., Reiff, E., Suprenant, K., Georg, G., and Himes, R. (2002) Epothilone and paclitaxel: Unexpected differences in promoting the assembly and stabilization of yeast microtubules. *Biochemistry 41*, 3870−3874.

(30) Anders, K. R., and Botstein, D. (2001) Dominant-lethal $\alpha$-tubulin mutants defective in microtubule depolymerization in yeast. *Mol. Biol. Cell 12*, 3973−3986.

(31) Reijo, R. A., Cooper, E. M., Beagle, G. J., and Huffaker, T. C. (1994) Systematic mutational analysis of the yeast $\beta$-tubulin gene. *Mol. Biol. Cell 5*, 29−43.

(32) Richards, K. L., Anders, K. R., Nogales, E., Schwartz, K., Downing, K. H., and Botstein, D. (2000) Structure-function relationships in yeast tubulins. *Mol. Biol. Cell 11*, 1887−1903.
(33) Joel, P. B., Fagnant, P. M., and Trybus, K. M. (2004) Expression of a nonpolymerizable actin mutant in Sf9 cells. *Biochemistry 43*, 11554−11559.
(34) Ducka, A. M., Joel, P., Popowicz, G. M., Trybus, K. M., Schleicher, M., Noegel, A. A., Huber, R., Holak, T. A., and Sitar, T. (2010) Structures of actin-bound Wiskott-Aldrich syndrome protein homology 2 (WH2) domains of Spire and the implication for filament nucleation. *Proc. Natl. Acad. Sci. U.S.A. 107*, 11757−11762.
(35) Nair, U. B., Joel, P. B., Wan, Q., Lowey, S., Rould, M. A., and Trybus, K. M. (2008) Crystal structures of monomeric actin bound to cytochalasin D. *J. Mol. Biol. 384*, 848−864.
(36) Rould, M. A., Wan, Q., Joel, P. B., Lowey, S., and Trybus, K. M. (2006) Crystal structures of expressed non-polymerizable monomeric actin in the ADP and ATP states. *J. Biol. Chem. 281*, 31909−31919.
(37) Li, H., DeRosier, D. J., Nicholson, W. V., Nogales, E., and Downing, K. H. (2002) Microtubule structure at 8 Å resolution. *Structure 10*, 1317−1328.
(38) Nogales, E., Whittaker, M., Milligan, R. A., and Downing, K. H. (1999) High-resolution model of the microtubule. *Cell 96*, 79−88.
(39) Nogales, E., Wolf, S. G., and Downing, K. H. (1998) Structure of the $\alpha\beta$ tubulin dimer by electron crystallography. *Nature 391*, 199−203.
(40) Maddox, P. S., Bloom, K. S., and Salmon, E. D. (2000) The polarity and dynamics of microtubule assembly in the budding yeast *Saccharomyces cerevisiae*. *Nat. Cell Biol. 2*, 36−41.
(41) Nettles, J. H., Li, H., Cornett, B., Krahn, J. M., Snyder, J. P., and Downing, K. H. (2004) The binding mode of epothilone A on $\alpha,\beta$-tubulin by electron crystallography. *Science 305*, 866−869.